Mathematical Biosciences and Engineering

https://www.aimspress.com/journal/mbe

MBE, 23(8): 2429–2461.
DOI: 10.3934/mbe.2026088
Received: 13 April 2026
Revised: 28 June 2026
Accepted: 20 July 2026
Published: 07 August 2026

Research article

Modeling cancer dynamics in an inflammatory environment

Rachid Ouifki[1,*], **Evans Afenya**[2] **and Suneel Mundle**[3]

[1] School of Mathematical and Statistical Sciences, PAA Research Entity, North-West University, South Africa

[2] Department of Mathematics, Elmhurst University, 190 Prospect Ave, Elmhurst, IL 60126, USA

[3] Department of Biochemistry, Rush University Medical Center, 1735 W. Harrison St, Chicago, IL 60612, USA

* **Correspondence:** Email: Rachid.Ouifki@nwu.ac.za; ouifkir@gmail.com.

Abstract: The phenomenon of inflammation is increasingly being implicated as a promoter of cancer development. Accordingly, linkages between different cancer types and inflammation are traced. Findings in the biomedical literature related to inflammatory footprints in cancer development are highlighted. Existing mathematical models, even though few, that involve inflammation and cancer are reviewed. With emphasis on the need for increased modeling activity in the area, the biomedical discussions and modeling reviews then lead into the proposal of a simple mathematical model that serves as an additional candidate model for studying cancer dynamics in an inflammatory environment. This is looked at as a way of building upon the relatively few mathematical modeling approaches that may be useful for providing insights as the biomedical studies and investigations proceed. The proposed model consists of a system of three ordinary differential equations tracking the interaction dynamics of cancer cells, inflammatory cells, and normal tissue. Subsequently, model steady states are analyzed and most importantly given necessary interpretations in biomedical contexts. To address parameter variability, uncertainty analysis using Latin Hypercube sampling is used to explore output uncertainty, while partial rank correlation coefficient (PRCC) sensitivity analysis identifies key driving parameters. PRCC analysis identifies three immunologically distinct pathways: one drives a protective anti-tumor response, promoting inflammatory cells that suppress cancer while sparing normal tissue; another drives tumor expansion and tissue damage while dampening inflammation, suggesting a pathogenic role; and a third supports normal tissue maintenance but indirectly fuels cancer growth and may limit inflammatory cells via resource competition. These findings underscore the challenge of supporting normal tissue without inadvertently fueling cancer growth.

Keywords: Normal cells; cancer cells; inflammation; mathematical models

1. Introduction

Research at the interface of three broad disciplines, namely, the fields of biology, medicine, and mathematics, has been gradually developing over the past few decades. Within this scheme, a role is increasingly bestowed on mathematical modeling as a tool that could be used to gain insight into certain important intricacies of observed and hidden behaviors in biological and medical systems, particularly in non-invasive ways. The employment and deployment of mathematical modeling becomes more important as biomedicine gains an increasingly quantitative status and posture. Mathematical modeling may help in various ways to prevent and avoid risky experiments and seemingly dangerous biomedical investigative processes. Among the many challenges confronting biomedicine, our focus in this article will be on the area encompassing the phenomenon of inflammation as it relates to cancer. Inflammation appears to have been ignored for many years but has seen, in the last few decades, growing levels of investigations that we believe could be further enhanced with the use of the quantitative tools of mathematical modeling. Within this framework, we proceed to first perform a review of some representative studies of inflammation and cancer and then look at how mathematical modeling has been employed in studying these phenomena in recent times.

1.1. Biomedical overview

Inflammation can be characterized as a complex biological response of the immune system to harmful stimuli due to damaged cells or irritants. Over 150 years ago, Rudolf Virchow provided the first indication of a possible link between inflammation and cancer. Yet, it is only during the last one to two decades that clear evidence has been obtained that inflammation plays a critical role in tumorigenesis and that some of the underlying molecular mechanisms have been elucidated [22]. A role for inflammation in tumorigenesis is now generally accepted, and it has become evident that an inflammatory microenvironment is an essential component of all tumors, including a few cases in which a direct causal relationship with inflammation is not yet proven [27]. Blaylock [10] posits that the main cause of malignancy comes from inflammation and cancer stem cells (CSCs). Accordingly, it is discernible that inflammation is essential to not only cancer induction by its mutagenic effects on stem cell DNA but also that the subsequent long term behavior of tumors is, to a large degree, determined by the tumor's microenvironment [25] that happens to be itself inflammatory.

The inflammatory microenvironment is essential to malignant transformation and the subsequent biological behavior of cancers, and this makes mere stimulation of cell proliferation, as was previously thought, insufficient for cancer development [12]. This inflammatory milieu in the microenvironment remains in the vicinity of cancer cells throughout the malignant process and the degree of inflammation appears to determine the proliferative potential of the tumor, as well as its invasive and metastatic aggressiveness [43]. What we learn then from various studies is that inflammation is central to all cancers and the cell processes involved in inflammation are not only responsible for initiation of the cancer but also persist during its growth and play a central role throughout every phase of the cancer's existence, including progression, invasion, angiogenesis, and metastasis [27, 33]. The cancer itself is a source of inflammation because of its antigenicity and destruction of healthy cells. Additionally, inflammatory mediators within the tumor microenvironment provide the tumor with the properties of "immune invisibility" and what essentially arises is a transformation of stem-like cells into immortal cancer stem cells followed by their subsequent long-term production of additional inflammation by generating cytokines

and chemokines, with pro-inflammatory cytokines, such as tumor necrosis factor-alpha, up-regulating the expression of chemokine receptors [23]. Because the tumor itself is antigenic and is releasing chemokines (immune cell attractants), it attracts an additional array of immune cells into the tumor's microenvironment as well. This creates a tumor microenvironment that is inflammatory throughout the life of the tumor [10].

Grivennikov et al. [18] have also pointed out that inflammatory responses play decisive roles at different stages of tumor development, including initiation, promotion, malignant conversion, invasion, and metastasis. Inflammation also affects immune surveillance and responses to therapy. They have revealed that immune inflammatory cells that infiltrate tumors engage in an extensive and dynamic crosstalk with cancer cells and some of the molecular events that mediate this dialog. Such inflammatory cells can release chemicals of the reactive oxygen species that are actively mutagenic for nearby cancer cells thus accelerating their genetic evolution toward heightened states of malignancy. This suggests that inflammation is a core enabling agent in cancer development and the cells directly responsible for this enabling agent are largely the immortal CSCs [19], again showing the links between inflammation and cancer. Notably, CSCs were initially implicated in the pathogenesis of hematopoietic malignancies, such as myeloid leukemias [39, 11], and then years later were identified in solid tumors, such as breast carcinomas [5, 17]. CSCs may by themselves represent a double-threat, in that they are more resistant to therapeutic killing and, at the same time, are endowed with the ability to regenerate a tumor before, during, or after therapy [10]. The tumor-promoting capabilities of CSCs, coupled with the tumor-enhancing properties of inflammatory cells may combine to pose potent challenges in the diseased environment.

Continuing further, Shigdar *et.al*. [42] point out that cytokines, secreted by tumor associated immune cells, activate the necessary pathways required by CSCs to facilitate their progression through the epithelial-mesenchymal transition (EMT) and migration to distant sites. Once in situ, these CSCs are able to secrete their own attractants, thus providing an environment whereby these cells can continue to propagate the cancer in a secondary niche. In [8], Behranvand and coworkers argue that inflammation may show two opposite roles in the tumor microenvironment. On the one hand, inflammation, as an innate immune response, tries to suppress tumor growth but on the other hand, it might not be powerful enough to eradicate the cancer cells but rather provide appropriate conditions for cancer promotion and eventual relapse when treatment is carried out. Horning in on the fact that cancer can be categorized into the two broad areas of solid tumor cancers such, as breast and pancreatic carcinomas, and disseminated cancers, such as myelomas and leukemias, we notice that no matter the cancer in focus, inflammation, along with active CSC involvement and participation, plays an important role in cancer promotion and propagation. For example, Jeong et al., in [21], found out that the CD44+/CD24- (CSC) phenotype was significantly associated with intratumoral inflammation and tumor-infiltrating CD4+ T cell counts. Notably, tumor-infiltrating CD4+ T cells were significantly increased in patients with the basal-like molecular subtype of breast cancer. In their study, [21], they conclusively identified a significant association between inflammation and the CSC phenotype in breast cancer.

With regards to cancers of the disseminated type, the works in [19, 37, 38, 41, 24] suggest that even though inflammation has not received adequate recognition, it may create a maladaptive context in which bone marrow (BM) niche dysfunction occurs in conditions that promote genomic instability and potentially lead to the acquisition of somatic mutations and impaired normal hematopoiesis. Malignant mutations may then have increased potential to expand and evolve. In such contexts, in-

flammation may function as an initiator, as well as a driver, of hematological malignancies such as, acute myeloiid leukemia (AML), and other malignant diseases. All these again point to the importance of inflammation in cancer development.

The discussions so far give an indication of the growing body of biomedical knowledge that is being built in attempts to uncover the crucial linkages between inflammation and cancer. What is becoming clear from a biomedical viewpoint is that a critical mechanism that was correctly recognized over 150 years ago may have been overlooked and this touches mainly on the fact that inflammation is at the center of the cancer process. Also overlooked may be the fact that not all cells can become cancer rather, stem cells appear to be the major cell type involved in the development [10]. At this juncture, in the interest of brevity, it is necessary for us to move on to other segments of this article that form the focal points of this diction. Indeed, there are a host of other scientific articles that address our current subject matter, and some are mentioned in the references ([47]–[20]).

1.2. Review of mathematical models

As the biomedical studies of inflammation and cancer proceed, we believe that the important resource of mathematical modeling could be used to probe some of the intricate linkages and ensuing dynamics. Bearing in mind that mathematical modeling in this area has been very limited, we will proceed to discuss the few mathematical modeling works with the view to adding our modeling insights that may shed light on some of the intricacies in observations emerging from the biomedical findings. In [7], Andersen et al. discuss the chronic Philadelphia-negative myeloproliferative neoplasms (MPNs) that are acquired stem cell neoplasms which may ultimately get transformed into AML.They point to the role chronic inflammation plays as an important factor in the development and progression of MPNs from an early cancer stage to the advanced myelofibrosis stage and note that only a few studies exist that use mathematical models to describe the development of MPNs. Further, as we noted earlier, they observe that among the few mathematical modeling studies, none have addressed the role of inflammation in clonal evolution and disease progression.

In their work [7], they propose a mathematical model consisting of six compartments: the hematopoietic stem cells (HSC), hematopoietic mature cells (HMC), MPN-mutated stem cells (MPN SC) and MPN mature cells (MPN MC), with the HSC and HMC being normal cells and the MPN SC and MPN MC being the abnormal ones. The other two compartments include those of all dead cells denoted by a and the other represents an inflammatory level denoted by s. The model dynamics are described by a system of four nonlinear ordinary differential equations (ODEs) obeyed mainly by the HSC, HMC, MPN SC, and MPN MC, in a first case and in a second case by the full compendium consisting of HSC, HMC, MPN SC, MPN MC, a, and s. The two model sets are considered to represent specific phases. The first model of four ODEs that include HSC, HMC, MPN SC, and MPN MC dynamics do not account for niche feedback and inflammatory feedback related to cell mortality, and basically constitute the model proposed by Dingli and Michor [13], while the second model of all the six ODEs made up of HSC, HMC, MPN SC, MPN MC. a, and s do include the initially omitted characteristics. Essentially the modeling process describes the proliferation of stem cells into mature ones with inclusion of mutations of healthy stem cells into malignant ones. Regulatory interactions, such as niche growth effects and inflammation coping with cell death, inflammatory cytokines, and neutrophils, are included. The model is calibrated through the search for various model parameter values that the authors consider to be tantamount to model validation. Even though the authors did

not perform regular stability analysis of their full model, sensitivity analysis with regards to the model parameter space show that the parameters with the highest impact on model output are self-renewal and death rates of the HSC and MPN SC along with their associated inflammatory levels. Simulations of the model show that increased inflammation increases disease development and lower inflammatory levels make disease progression less rapid. On the bases of work done in the model [7], the authors conclude, and rightly so, based on all other considerations, that chronic inflammation is closely linked to the development of the myeloproliferative cancers.

We must mention here that mathematical modeling studies are relatively few in the literature apparently because this phenomenon had not been given much attention in the community in the past even though it had been of importance. Of the few that exists, and in addition to the one we just discussed [7], we review some by noting that in [15], Dunster and coworkers develop a spatially averaged model of inflammation that accounts for populations of neutrophils and macrophages and incorporate both pro- and anti-inflammatory processes. The resulting differential equations then exhibit two outcomes that they relate to healthy and unhealthy states. They use bifurcation analysis to investigate how variation in the system parameters affect system outcomes. They find that therapeutic manipulation of the rate of macrophage phagocytosis can aid in resolving inflammation but success is critically dependent on the rate of neutrophil apoptosis. Their model predicts that an effective treatment protocol would take a dual approach, targeting macrophage phagocytosis alongside neutrophil apoptosis.

Considering further representative models on inflammation and cancer, in [40], observing a tight coupling between inflammation and blood cancer, such as the myeloproliferative neoplasms (MPNs), the authors use a six-dimensional model that they call the Cancitis model to describe and analyze the progression of blood cancer coupled to the inflammatory system. They provide criteria for the existence of physiological steady states, such as the trivial, hematopoietic, malignant, and co-existing steady states. They classify the steady states in terms of the inflammatory stimuli and point out how several parameters play crucial roles in determining the attracting steady state(s). They note in particular that increasing inflammatory stimuli may transform a healthy state into a malignant state under certain conditions. In contrast however, for the co-existing steady state, increasing inflammatory stimuli may reduce the malignant cell burden. They conclude by pointing out that their model may provide an overview of the possible dynamics necessary in clinical practice for the use of inflammatory inhibitors during treatment. We note at this point that even though models of inflammation are relatively few, we point, for the sake of brevity and based on their similarity to what we have already discussed, to some works in the literature that the reader may find useful, [15, 40, 34, 31].

While the above-mentioned models explored tumor-immune dynamics within the context of inflammation, they did not appear to focus explicitly on inflammation's dual role in both promoting early tumor growth and mediating anti-tumor responses. Our work addresses, in a significant way, that gap, by proposing a tractable model that yields biologically meaningful insights.

At this juncture, we must mention that the biomedical literature is replete with diverse inflammation studies and part of our approach in these opening sections is to use the mentioned representative studies to most importantly motivate and seek justifications for our investigations from a biomathematical viewpoint. In our work, as described in the ensuing sections, we explicitly try to uncover the dynamics that arise when diseased or malignant cells and healthy or normal cells directly interact with immune inflammatory cells with these cells obeying generalized growth laws. Such generalized density-dependent growth laws lend themselves to the fact that cell populations such as, malignant

cell populations, cannot grow unboundedly in a human host without causing fatal damage to the host. Accordingly, in the bone marrow for example, hematopoietic cells may go through a process of rapid exponential growth at low population sizes and then later in the temporal continuum exhibit deceleration in their growth at large population sizes. Such growth behavior engenders sigmoidal growth characteristics that is reflected in our work and provides biological underpinnings and justification for our proposed model. Obviously, our approaches in this work find significance and importance in the spirit of the Norton-Simon hypothesis [32] that was formulated a number of decades ago and is still relevant in present biomedical studies. Upon these bases, we most importantly investigate the crucial parameters that play crucial roles in driving malignancy and give information to the clinician about system parameters that could be ignored in possible therapeutic situations.We must note here, though, that our specific modeling tasks in this discourse has been to present and study a candidate model that captures the behavior in the interactions between normal, abnormal, and immune inflammatory cells. Work on behaviors and implications that may arise in possible therapeutic settings will follow in a sequel to this article.

1.3. Aim and scope of the present study

The aim of this study is to develop and analyze a mathematical model capturing interactions between cancer cells, inflammatory cells, and normal tissue within the tumor microenvironment. We explore inflammation's dual role in both promoting early tumor growth and mediating anti-tumor responses. For this, we formulate a system of three ordinary differential equations tracking cancer, inflammatory, and normal cell dynamics. We analyze steady states and interpret their biological significance and perform uncertainty analysis using Latin Hypercube sampling along with partial rank correlation coefficient (PRCC) sensitivity analysis to identify key parameters driving system behavior. Finally, we interpret findings in the context of biomedical literature, distinguishing pro- from anti-tumorigenic inflammatory pathways. By integrating modeling with biological interpretation, this study aims to offer insights that may inform therapeutic strategies targeting inflammation in cancer.

2. Materials and methods

Employing all relevant information from the biomedical and mathematical modeling literature on inflammation as expressed in the collection of cited articles and existing work, we proceeded to first provide motivations for our work that engendered a candidate mathematical model that could be used to capture inflammatory dynamics. After that, we went on, using biomedical information assembled, to formulate the model that directly resulted from the inflammatory phenomena under study. We then fine-tuned the emerging model through further appraisal and design in what follows.

2.1. Model motivation, assumptions, formulation, and design

Following from our earlier discussions, we proceed to enumerate our motivations and assumptions that stem from biomedical information and data in the available literature.

1. Normal cells are assumed to grow according to a general density-dependent growth law that captures the biological fact that cell systems have asymptotic limits to their growth.

2. Cancer cells exhibit normal cell characteristics by also obeying similar growth law. Even though the appearance of such cells signify a diseased state in which uncontrollable growth of cells takes place, the geometry of the growth environment does biologically induce an asymptotic bound on growth.

3. Immune inflammatory cells stimulate the proliferation of normal cells through the action of various cytokines. In stimulating normal cell proliferation, these cytokines aid the normal cells to perform their important functions of guaranteeing homeostasis.

4. Immune inflammatory cells are modified by cancer cells in the inflammatory environment to anomalously stimulate their proliferation.

5. Through various biological mechanisms, normal cells mutate into cancerous cells.

6. Due to the inflammatory tumor microenvironment, normal healthy cells anomalously suffer inhibition from the immune inflammatory cells. They also encounter inhibition from the cancer cells that tend to replace them.

7. Cancerous cells may be enhanced by their interactions with immune cells while getting inhibited to some degree by these same immune cells.

Based on these assumptions, we let the following quantities represent the various different cell populations:

- N : Population of normal healthy body cells
- L : Population of cancer cells
- M : Population of immune cells with inflammatory properties

The ensuing model system that stands out among a number of candidates and captures the appropriate inflammatory dynamics is as follows:

$$\begin{cases} \frac{dN}{dt} = r_n N\rho(N+L+M) + \frac{\sigma_n NM}{C+M} - \alpha(M)N \\ \frac{dL}{dt} = r_l L\rho(N+L+M) + \frac{\sigma_l LM}{C+M} + \alpha(M)N \\ \frac{dM}{dt} = r_m M\rho(N+L+M) + \frac{\sigma_m LM}{C+M} \end{cases} \tag{2.1}$$

where

- $\rho : (0,\infty) \to \mathbb{R}$ is continuously differentiable, strictly decreasing, and satisfies

$$\lim_{T\to 0^+} \rho(T) > 0 \quad (\text{possibly } +\infty), \qquad \lim_{T\to\infty} \rho(T) = -\infty.$$

  This guarantees the existence of a unique carrying capacity $K > 0$ such that $\rho(K) = 0$, with $\rho(T) > 0$ for $T < K$ and $\rho(T) < 0$ for $T > K$, and $\rho'(K) < 0$. Typical choices of the function ρ include the logistic function $\rho(T) = 1 - \frac{T}{K}$, the generalized logistic function $\rho(T) = 1 - \left(\frac{T}{K}\right)^{\theta}, \theta > 0$, and the Gompertz function $\rho(T) = \ln\left(\frac{K}{T}\right)$.

- $\alpha : [0, \infty) \to \mathbb{R}$ is continuously differentiable and satisfies

$$\alpha(M) = \begin{cases} 0, & \text{if } M < M_c \\ \text{a monotonically increasing function with } \alpha(M_c) = 0, & \text{if } M \geq M_c \end{cases}$$

The chosen form captures three key features of inflammation-driven carcinogenesis: (i) a threshold level of inflammation below which repair and immune surveillance prevent malignant transformation, (ii) enhanced malignant transformation as inflammation-induced damage accumulates, and (iii) saturation at high inflammation levels due to limited inflammation-induced transformation.

It is important to note that biological justification of Model system (2.1) was given towards the end of last section. This touched on the fact that cell populations cannot grow unboundedly as fully supported by the biology behind the Norton-Simon hypothesis [32]

3. Results and interpretations

We now employ analytical techniques to uncover various scenarios that arise as a result of our modeling processes. We start by establishing the well-posedness of the model, then explore its dynamics in the absence of inflammation and then followed by the case when inflammation is present.

3.1. Model well-posedness

In this subsection, we investigate the well-posedness of system (2.1) by establishing the positivity and boundedness of its solutions, thereby ensuring their biological feasibility.

Theorem 1. *For given $N(0) \geq 0$, $L(0) \geq 0$ and $M(0) \geq 0$, the solutions $N(t)$, $L(t)$ and $M(t)$ of system* (2.1) *exist and remain non-negative for all $t \geq 0$.*
Choose $\eta > \frac{\sigma}{r_1}$, where $r_1 = \max(r_n, r_l, r_m)$ and $\sigma = \max(\sigma_n, \sigma_l + \sigma_m)$, and define

$$\bar{T} := \inf\{T \geq 0 : \rho(S) \leq -\eta \quad \text{for all } S \geq T\}.$$

Then, the domain

$$\mathcal{D} = \left\{(N, L, M) \in \mathbb{R}^3_+ : \ N + L + M \leq \bar{T}\right\},$$

is positively invariant under the flow of system (2.1).

Proof. The existence and uniqueness of the model's solutions are standard and follow from classical results in the theory of ordinary differential equations. The non-negativity of $N(t)$ and $L(t)$ is obtained through direct integration of their respective equations in (2.1), that is,

$$N(t) = N(0)e^{\int_0^t \left(r_n\rho(N(s)+L(s)+M(s))+\frac{\sigma_n M(s)}{C+M(s)}-\alpha(M(s))\right)ds}$$

$$M(t) = M(0)e^{\int_0^t \left(r_m\rho(N(s)+L(s)+M(s))+\frac{\sigma_m L(s)}{C+M(s)}\right)ds}$$

The non-negativity of $L(t)$ follows from the non-negativity of $N(t)$ and $M(t)$ together with the variation-of-constants formula

$$L(t) = L(0)\mathcal{U}(t, 0) + \int_0^t \mathcal{U}(t, s)\alpha(M(s))N(s)ds$$

where $\mathcal{U}(t,s) = e^{\int_s^t \left(r_l\rho(N(\tau)+L(\tau)+M(\tau))+\frac{\sigma_l M(\tau)}{C+M(\tau)}\right)d\tau}$.

We shall next establish that the domain $\mathcal{D}$ is positively invariant under the flow of system (2.1). Denote by $T(t) = N(t) + L(t) + M(t)$ and $T_0 = T(0)$. Adding together the equations of (2.1) leads to

$$\begin{aligned}\frac{dT}{dt} &= (r_n N + r_l L + r_m M)\rho(T) + \frac{\sigma_n NM + (\sigma_l+\sigma_m)LM}{C+M} \\ &\leq r_1 T\rho(T) + \sigma T.\end{aligned}$$

Since $\limsup_{T\to\infty}\rho(T) = -\infty$, then for all $\eta > \frac{\sigma}{r_1}$, we have

$$\limsup_{T\to\infty}\rho(T) < -\eta < -\frac{\sigma}{r_1}. \tag{3.1}$$

Now define

$$\bar{T} := \inf\{T \geq 0 : \rho(S) \leq -\eta \quad \text{for all } S \geq T\}.$$

$\bar{T}$ exists and is finite because the set is nonempty (by (3.1)) and bounded below by 0. By the definition of infimum and the continuity of ρ, we have for all $T \geq \bar{T}$,

$$\rho(T) \leq -\eta.$$

Consequently, for $T \geq \bar{T}$, we get

$$\frac{dT}{dt} \leq r_1 T(-\eta) + \sigma T = T(\sigma - r_1\eta),$$

where $\sigma - r_1\eta < 0$ because $-\eta < -\frac{\sigma}{r_1}$.

Take any initial condition with $T(0) \leq \bar{T}$ and suppose, for contradiction, that there exists a first time $t_1 > 0$ such that $T(t_1) > \bar{T}$. By continuity, there is a time $t^* \in (0, t_1]$ such that $T(t^*) = \bar{T}$ and $\frac{d}{dt}T(t^*) \geq 0$ (since the trajectory crosses the threshold from below). However, at $T = \bar{T}$, we have

$$\frac{d}{dt}T(t^*) \leq T(t^*)(\sigma - r_1\eta) < 0.$$

which is a contradiction. Hence, $T(t) \leq \bar{T}$ for all $t \geq 0$. Thus $(N(t), L(t), M(t)) \in \mathcal{D}$ for all $t \geq 0$. This completes the proof. □

Remark 2. In the logistic case $\rho(T) = 1 - T/K$, the total population satisfies the quadratic differential inequality

$$\frac{dT}{dt} \leq (r_1 + \sigma)T - \frac{r_2}{K}T^2,$$

which yields the standard bound

$$T \leq \frac{(\sigma + r_1)K}{r_2}, \quad r_2 = \min(r_n, r_l, r_m).$$

The general invariance theorem recovers this same bound by choosing

$$\eta = \frac{\sigma}{r_1} + (\sigma + r_1)\left(\frac{1}{r_2} - \frac{1}{r_1}\right).$$

Indeed, solving $\rho(\bar{T}) = -\eta$ gives $\bar{T} = K(\sigma + r_1)/r_2$, so the invariant domain is

$$\Omega = \left\{(N, L, M) \in \mathbb{R}^3_+ : N + L + M \leq \frac{(\sigma + r_1)K}{r_2}\right\}.$$

3.2. Equilibrium points and stability behavior

The equilibrium points of model (2.1) are determined by solving the following algebraic system, obtained by setting the right-hand side of (2.1) to zero, and identifying its non-negative solutions.

$$\begin{cases} \left(r_n\rho(N+L+M)+\frac{\sigma_n M}{C+M}-\alpha(M)\right)N=0 \\ r_l L\rho(N+L+M)+\frac{\sigma_l LM}{C+M}+\alpha(M)N=0 \\ \left(r_m\rho(N+L+M)+\frac{\sigma_m L}{C+M}\right)M=0 \end{cases} \tag{3.2}$$

Proposition 3. *The trivial point $E_0=(0,0,0)$ is always an equilibrium point of (2.1) and is unstable.*

3.2.1. Inflammation-free equilibrium points

In this section we investigate the inflammation-free equilibrium points of (2.1) by setting $M=0$ in (3.2) and exploring the non-negative solutions of the resulting system, that is,

$$\begin{cases} r_n\rho(N+L)N=0 \\ r_l\rho(N+L)L=0 \end{cases}$$

Using the fact that $\rho(T)=0$ if and only if $T=K$, we obtain the following equilibrium points:

1. $E_n=(K,0,0)$, which represents the scenario where there is no tumor or inflammation
2. $E_l=(0,K,0)$, which represents the scenario of full-blown cancer with no inflammation
3. $E_{nl}=(N,K-N,0)$, $N<K$ representing a family of equilibrium points where normal and tumor cells coexist in the absence of inflammation

Proposition 4. *The inflammation-free equilibrium points E_l and E_{nl} are unstable. Moreover,*

(a) If $-Kr_n\rho'(K)\sigma_l-r_l\sigma_n>0$, then E_n is unstable.

(b) If $-Kr_n\rho'(K)\sigma_l-r_l\sigma_n<0$, then E_n is locally asymptotically stable in the positive orthant $\mathbb{R}^3_+$.

Proof. Calculating the Jacobian matrices at these equilibrium points and using $\rho(K)=0$, we obtain:

1. At E_l, we have

$$J_{E_l}=\begin{bmatrix} 0 & 0 & 0 \\ Kr_l\rho'(K) & Kr_l\rho'(K) & K\left(r_l\rho'(K)+\frac{\sigma_l}{C}\right) \\ 0 & 0 & \frac{K\sigma_m}{C} \end{bmatrix}$$

   Since J_{E_l} has a positive eigenvalue given by $,\frac{K\sigma_m}{C}$, then E_l is unstable.

2. At $E_{nl}=(N,K-N,0)\,,N<K$, we have

$$J_{E_{nl}}=\begin{bmatrix} Nr_n\rho'(K) & Nr_n\rho'(K) & N\left(r_n\rho'(K)+\frac{\sigma_n}{C}\right) \\ r_l\rho'(K)(K-N) & r_l\rho'(K)(K-N) & \left(r_l\rho'(K)+\frac{\sigma_l}{C}\right)(K-N) \\ 0 & 0 & \frac{\sigma_m(K-N)}{C} \end{bmatrix}$$

   with a positive eigenvalue $\frac{\sigma_m(K-N)}{C}>0$. Hence, E_{nl} is unstable.

3. At E_n, we have

$$J_{E_n} = \begin{bmatrix} Kr_n\rho'(K) & Kr_n\rho'(K) & K\left(r_n\rho'(K) + \frac{\sigma_n}{C}\right) \\ 0 & 0 & 0 \\ 0 & 0 & 0 \end{bmatrix}$$

The Jacobian matrix at the equilibrium point, E_n has one negative eigenvalue $Kr_n\rho'(K)$ and two zero eigenvalues. Hence, J_{E_n} is nonhyperbolic and the linearization around E_n alone does not suffice to determine its stability. To investigate the stability of E_n, we employ the center manifold reduction technique [45].
Using the invariance property of a center manifold, system (2.1) is equivalent to the reduced system (5.5) derived in Appendix

$$\begin{cases} x_1' = \dfrac{x_1\left(-Kr_n\rho'(K)\sigma_m x_2 - r_m\sigma_n x_1\right)}{-Kr_n\rho'(K)(C + x_1)} \\ x_2' = \dfrac{x_1 x_2\left(-Kr_n\rho'(K)\sigma_l - r_l\sigma_n\right)}{-Kr_n\rho'(K)(C + x_1)}. \end{cases} \tag{3.3}$$

We distinguish two cases.

(a) If $-Kr_n\rho'(K)\sigma_l - r_l\sigma_n > 0$, then

$$x_2' = \frac{x_1 x_2(-Kr_n\rho'(K)\sigma_l - r_l\sigma_n)}{-Kr_n\rho'(K)(C + x_1)} > 0$$

for all $x_1, x_2 > 0$. Hence $x_2(t)$ is strictly increasing and therefore cannot converge to zero. Consequently, positive solutions cannot converge to $(0, 0)$.

(b) If $-Kr_n\rho'(K)\sigma_l - r_l\sigma_n < 0$, then for all solutions starting in a sufficiently small positive neighborhood of $(0, 0)$, we have $x_2' < 0$, so $x_2(t)$ is strictly decreasing. Since $x_2(t)$ is bounded below by zero, it converges to some limit $x_2^* \geq 0$. Moreover, let t_c be a critical point of x_1. Since $x_1'(t_c) = 0$, we have

$$x_1''(t_c) = \frac{\sigma_m x_1(t_c)x_2'(t_c)}{C + x_1(t_c)} < 0,$$

showing that x_1 has at most one critical point, and if it exists it is a strict local maximum. Therefore, x_1 is either

(i) monotonically increasing
(ii) monotonically decreasing
(iii) increasing and then decreasing, with at most one critical point

We first exclude case (i). Suppose that x_1 is monotonically increasing. Since $x_1(t)$ is bounded and increasing, it converges to some limit $x_1^* > 0$. Moreover, we have $x_1'(t) > 0$ for all t, which together with the first equation of (3.3), yields

$$-Kr_n\rho'(K)\sigma_m x_2 - r_m\sigma_n x_1 > 0. \tag{3.4}$$

Passing to the limit in (3.4) gives

$$-Kr_n\rho'(K)\sigma_m x_2^* - r_m\sigma_n x_1^* \geq 0.$$

Since $x_1(t)$ and $x_2(t)$ are both monotonic and converge, we have

$$\lim_{t\to\infty} x_1'(t) = 0, \qquad \lim_{t\to\infty} x_2'(t) = 0.$$

Passing to the limit in (3.3) yields

$$\begin{cases} \dfrac{x_1^*\left(-Kr_n\rho'(K)\sigma_m x_2^* - r_m\sigma_n x_1^*\right)}{-Kr_n\rho'(K)(C+x_1^*)} = 0, \\ \dfrac{x_1^* x_2^*\left(-Kr_n\rho'(K)\sigma_l - r_l\sigma_n\right)}{-Kr_n\rho'(K)(C+x_1^*)} = 0. \end{cases} \tag{3.5}$$

The second equation of (3.5) yields

$$x_1^* x_2^* = 0.$$

Since $x_1^* > 0$, then $x_2^* = 0$. Using the first equation of (3.5), we obtain $x_1^* = 0$, which contradicts $x_1^* > 0$. Therefore, case (i) is impossible.

Hence, only cases (ii) and (iii) remain. In either case there exists $t_1 > 0$ such that

$$x_1'(t) < 0, \qquad t > t_1.$$

Therefore, $x_1(t)$ is eventually monotone decreasing and bounded below, so

$$x_1^* := \lim_{t\to\infty} x_1(t) \geq 0.$$

Since $x_1'(t) < 0$ for all sufficiently large t, the first equation of (3.3) implies

$$-Kr_n\rho'(K)\sigma_m x_2 - r_m\sigma_n x_1 < 0$$

for all sufficiently large t. Passing to the limit gives

$$-Kr_n\rho'(K)\sigma_m x_2^* - r_m\sigma_n x_1^* \leq 0. \tag{3.6}$$

Passing to the limit in (3.3) again yields

$$x_1^* x_2^* = 0.$$

If $x_2^* = 0$, then from the first equation of (3.3) we obtain $x_1^* = 0$. If $x_1^* = 0$, then from (3.6) and using $x_2^* \geq 0$, we get $x_2^* = 0$. In both cases, every trajectory of the reduced system in a sufficiently small positive neighborhood of $(0, 0)$ converges to $(0, 0)$.
Hence, E_n is locally asymptotically stable in the positive orthant $\mathbb{R}^3_+$.

□

Proposition 4 indicates that when $-Kr_n\rho'(K)\sigma_l - r_l\sigma_n > 0$ system (2.1) cannot stabilize at an inflammation-free equilibrium, implying that inflammation will emerge and be established over time. The following analysis further investigates the persistence of inflammation and its potential role in sustaining cancer progression.

3.2.2. Equilibrium points with inflammation

In this section, we investigate the equilibrium points of system (2.1) corresponding to a positive inflammation level ($M > 0$). We establish the following result.

Proposition 5. *Let $E = (N, L, M)$ be an equilibrium point of system* (2.1) *with $M > 0$. Then, either $N = L = 0$, leading to $E_m = (0, 0, K)$ which is unstable , or N and L are both positive. In particular, if at equilibrium, both $M > 0$ and $N > 0$, then necessarily $L > 0$.*

Proof. 1. Suppose $N = 0$. From $(3.2)_2$ we obtain $r_l L\rho(L+M) = 0$, which implies $L = 0$ or $L+M = K$ (due to $\rho(T) = 0$ if and only if $T = K$). If $L + M = K$, then by $(3.2)_3$ we have $\dfrac{\sigma_m L}{C + M} = 0$ which yields $L = 0$.

2. Suppose $L = 0$. Then, from $(3.2)_3$ we obtain $r_m\rho(L + M) = 0$. Substituting into $(3.2)_2$ gives $\alpha(M)N = 0$ implying that $\alpha(M) = 0$ or $N = 0$. If $\alpha(M) = 0$, then from $(3.2)_1$ we have $\dfrac{\sigma_n M}{C + M}N = 0$, which (since $M > 0$) implies that $N = 0$, leading to $E_m = (0, 0, K)$. The Jacobian matrix at E_m is

$$J_{E_m} = \begin{pmatrix} \dfrac{\sigma_n K}{C + K} - \alpha(K) & 0 & 0 \\ \alpha(K) & \dfrac{\sigma_l K}{C + K} & 0 \\ r_m K\rho'(K) & r_m K\rho'(K) + \dfrac{\sigma_m K}{C + K} & r_m K\rho'(K) \end{pmatrix}.$$

Its eigenvalues are

$$\begin{cases} \lambda_0 = r_m K\rho'(K) < 0, \\ \lambda_1 = \dfrac{\sigma_l K}{C + K} > 0 \\ \lambda_2 = \dfrac{(K\sigma_n - (C + K)\alpha(K))}{C + K}. \end{cases} \tag{3.7}$$

Since $\lambda_1 > 0$, we conclude that E_m is unstable.

□

Remark 6. The biological implication of this result is that inflammation can destabilize the cancer-free equilibrium $(K, 0, 0)$, potentially enabling the initiation of cancer. Once cancer cells are present, inflammation may interact with both normal and cancer cells to sustain long-term interior equilibrium points $E = (N, L, M)$ with $0 < M, N, L \leq K$, which correspond to persistent cancer supported, at least in part, by chronic inflammation.

If $M \leq M_c$, we have $\alpha(M) = 0$ reducing system (3.2) to

$$\begin{cases} \left(r_n\rho(N + L + M) + \frac{\sigma_n M}{C+M}\right)N = 0 \\ \left(r_l\rho(N + L + M) + \frac{\sigma_l M}{C+M}\right)L = 0 \\ \left(r_m\rho(N + L + M) + \frac{\sigma_m N}{C+M}\right)M = 0. \end{cases} \tag{3.8}$$

Proposition 7. *If $r_l\sigma_n - r_n\sigma_l \neq 0$, then system* (2.1) *has no interior equilibrium with $M \leq M_c$.*

Proof. If $N > 0$ and $L > 0$, then system (3.8) reduces to

$$\begin{cases} r_n\rho(N+L+M) + \frac{\sigma_n M}{C+M} = 0 \\ r_l\rho(N+L+M) + \frac{\sigma_l M}{C+M} = 0 \\ \left(r_m\rho(N+L+M) + \frac{\sigma_m N}{C+M}\right) M = 0. \end{cases} \tag{3.9}$$

Dividing the first two equations of (3.9) by r_n and r_l, respectively, and subtracting gives

$$\left(\frac{\sigma_n}{r_n} - \frac{\sigma_l}{r_l}\right)\frac{M}{C+M} = 0.$$

Since $r_l\sigma_n - r_n\sigma_l \neq 0$, then $M = 0$, contradicting $M > 0$ for an interior equilibrium points. Hence, no interior equilibrium exists with $M \leq M_c$. □

This result has an important biological implication: if the maximum carrying capacity is smaller than the inflammation threshold M_c, that is,

$$\bar{T} < M_c,$$

then system (2.1) has no interior equilibrium point with $N > 0, L > 0$ and $0 < M \leq M_c$. Indeed, if $E = (N, L, M)$ is an interior equilibrium point, then $M \leq \bar{T}$. However, Proposition 7 yields $M > M_c$, implying that $M > \bar{T}$ which contradicts $M \leq \bar{T}$.

Biologically, this indicates that when the resources available within the tumor microenvironment are low, any inflammation that arises will inevitably subside, and the system will return to an inflammation-free state. However, inflammation may persist when the tumor burden potentially exceeds the critical threshold M_c. From a therapeutic perspective, this suggests that interventions aimed at reducing the effective carrying capacity below M_c, such as microenvironmental starvation, could help prevent chronic inflammation and thereby reduce the likelihood of cancer persistence.

When the maximum carrying capacity exceeds the inflammation threshold ($\bar{T} > M_c$), the investigation of interior equilibrium points with sustained inflammation, namely $E = (N, L, M)$ with $M_c < M \leq K$, becomes analytically complex. This difficulty arises primarily from the nonlinear structure of $\alpha(M)$. Consequently, a numerical investigation may be required.

3.3. Uncertainty and sensitivity analyses

Because of the uncertainty associated with their key parameters, it is essential to assess how these uncertainties may influence the model's outcomes, particularly cancer cells $L(t)$ and inflammation $M(t)$. In uncertainty and sensitivity analyses, we elect to use, among various candidates, the following function which is smooth enough and transitions from 0 to a desired maximum finite value in a smooth fashion.

$$\alpha(M) = \begin{cases} 0, & \text{if } M < M_c \\ \alpha_1\left(1 - e^{-\xi(M-M_c)^2}\right), & \text{if } M \geq M_c. \end{cases} \tag{3.10}$$

The exponential form was chosen as a smooth threshold function satisfying $\alpha(M) = 0$ for $M \leq M_c$ and increasing smoothly thereafter until saturation, thereby serving as a regular approximation of a biological switching mechanism. From a mathematical point of view, its smoothness ensures the applicability of classical well-posedness results and local analysis around equilibria.

To this end, we first perform Latin hypercube sampling (LHS) [29] to generate a representative sample of the parameter space. Next, we conduct a global uncertainty analysis to examine how variations in parameter values propagate through the model. Finally, we evaluate the influence of individual parameters on the model output by computing PRCC, following the methodology of Marino et al. [28].

3.3.1. LHS

We performed LHS with 5×10^4 realizations of the parameters $r_n, r_l, r_m, K, C, \sigma_m, \sigma_l, \alpha_1$, and M_c sampled within the ranges specified in Table 1.

Table 1. Description of the model's parameters.

Parameter	Description	Value	Range	Source/Reference
r_n	Proliferation rate of N cells	0.05	[0.002, 0.149]	[3, 4]
r_l	Proliferation rate of L cells	0.005	[0.0001, 0.05221]	[3, 4, 1]
r_m	Proliferation rate of M cells	1	[0.015, 2]	[7, 2]
K	Carrying capacity	1×10^{13}	$[10^{12}, 3.688 \times 10^{14}]$	[3, 4, 2, 1]
C	Half-saturation constant	1×10^6	$[10^5, 2 \times 10^6]$	Assumed
σ_n	Interaction coefficient for N	0.15	[0.048, 0.24]	Assumed
σ_l	Interaction coefficient for L	0.08	[0.024, 0.12]	Assumed
σ_m	Interaction coefficient for M	0.03	[0.024, 0.048]	Assumed
α_1	Transition rate scaling factor	0.2	[0.1, 0.3]	Assumed
ξ	Sharpness of transition at M_c	10	[5, 20]	Assumed
M_c	Critical threshold for M	1×10^8	$[10^6, 10^7]$	Assumed

Subsequently, we examined the pairwise associations between parameters using Pearson correlation coefficients to assess linear relationships [35], and Spearman correlation coefficients to detect nonlinear monotonic relationships between the sampled parameters [44]. The resulting scatter plots of the sampled parameters, along with the corresponding correlation coefficients and their associated p-values are shown in Figure 6 in the appendix. They reveal that the Pearson and Spearman correlation coefficients among the sampled parameters are very small, which, according to the classification of correlation strengths in [46], falls within the "poor" range. Moreover, all associated p-values exceed the 5% significance threshold, indicating that even these weak correlations are not statistically significant and are likely attributable to random variation.

Overall, the low magnitude of the correlation coefficients combined with non-significant p-values indicates that no strong or statistically significant correlations exist among the LHS-generated samples, confirming their suitability for subsequent uncertainty analysis.

3.3.2. Uncertainty analysis

In this section, we assume that the cell population dynamics follow a logistic growth law and perform a global uncertainty analysis using the LHS samples described above, with parameter values from Table 1 and initial conditions $N(0) = 10^{12}$, $L(0) = 10^3$, and $M(0) = 10^3$. For each parameter realization, we evaluate the model variables and compute the mean solution along with the corresponding 95% uncertainty intervals, providing a quantitative measure of the variability induced by parameter uncertainty. The results are presented in Figures 1–3.

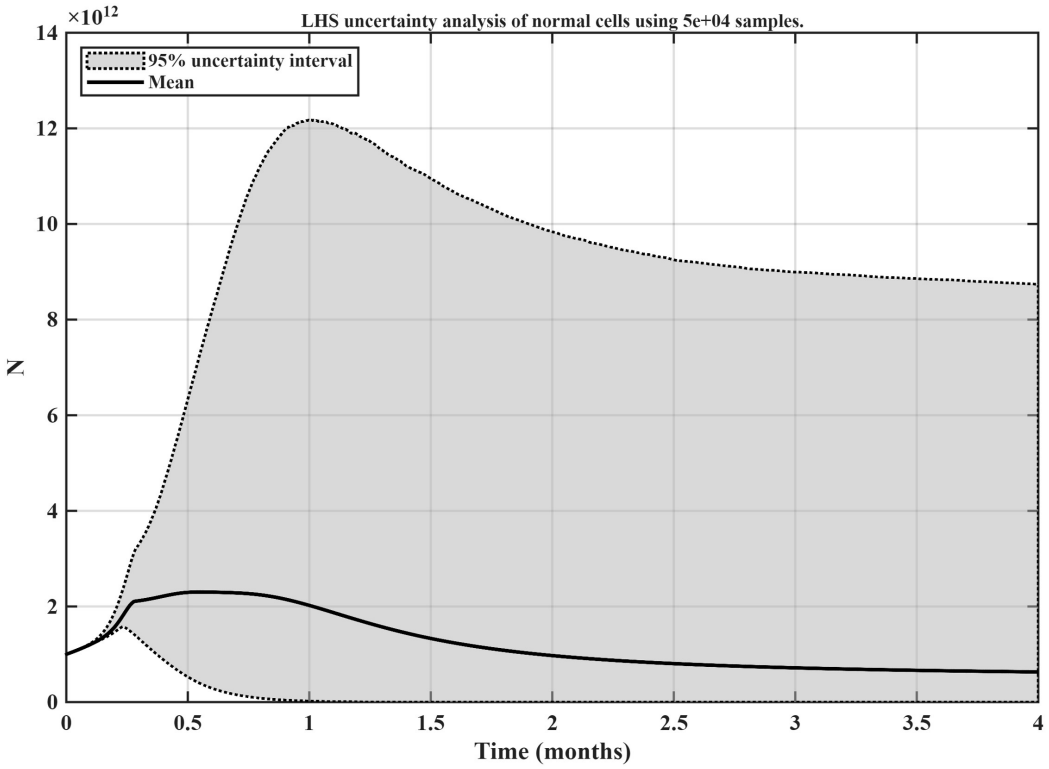

Figure 1. Temporal evolution of normal cells (N) for the 5×10^4 LHS sampled parameters.

Figure 1 shows that normal cell populations initially increase slightly before gradually declining. This pattern suggests that normal tissue levels are initially maintained but become progressively compromised as cancer and inflammation develop. The decline in normal cells could result from competition for limited resources with tumor (L) and inflammatory (M) cells, or from the positive effect of inflammation, $\sigma_n NM/(C + M)$, being dominated by the inhibitory term $\alpha(M), N$. The wide range of uncertainty reflects variability in parameters, such as baseline proliferation and susceptibility to damage.

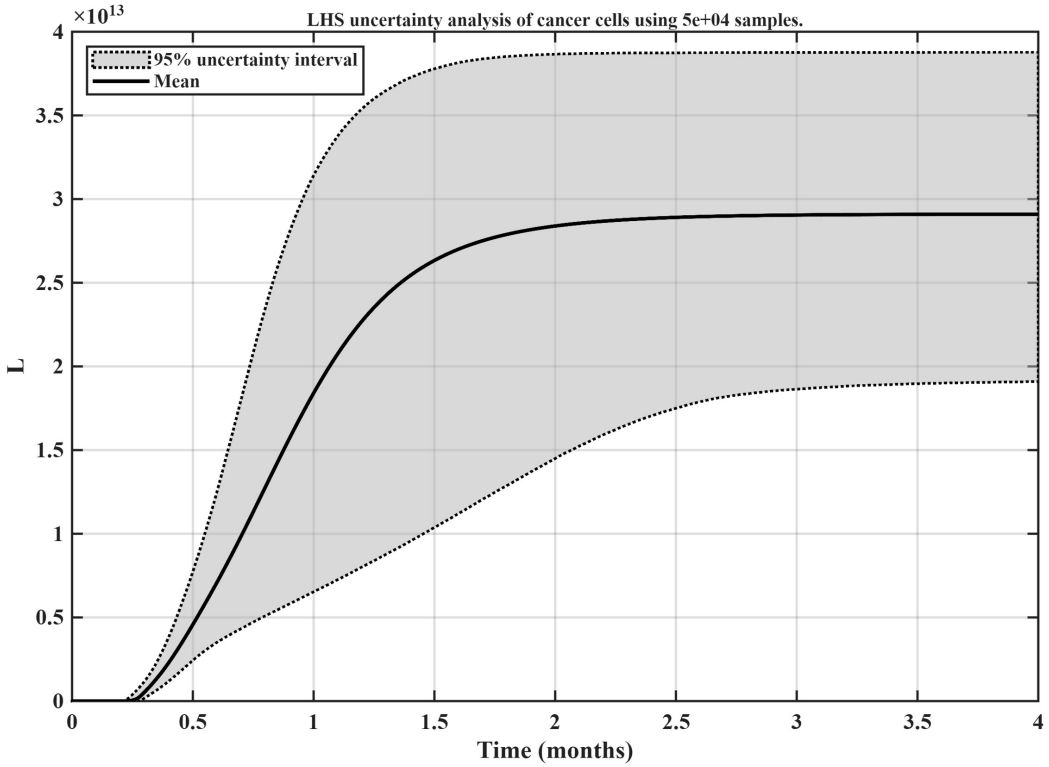

Figure 2. Temporal evolution of cancer cells (L) for the 5×10^4 LHS parameters.

Figure 2 shows that the mean cancer cell population rises sharply during the first 1–2 months before plateauing around 3×10^{13}. This pattern reflects rapid early tumor growth driven by uncontrolled proliferation, followed by saturation likely resulting from competition with normal and inflammatory cells for limited space and nutrients within the tumor microenvironment. The 95% uncertainty interval is initially wide but narrows over time, indicating that despite parameter variability, the final tumor size becomes relatively predictable once growth stabilizes.

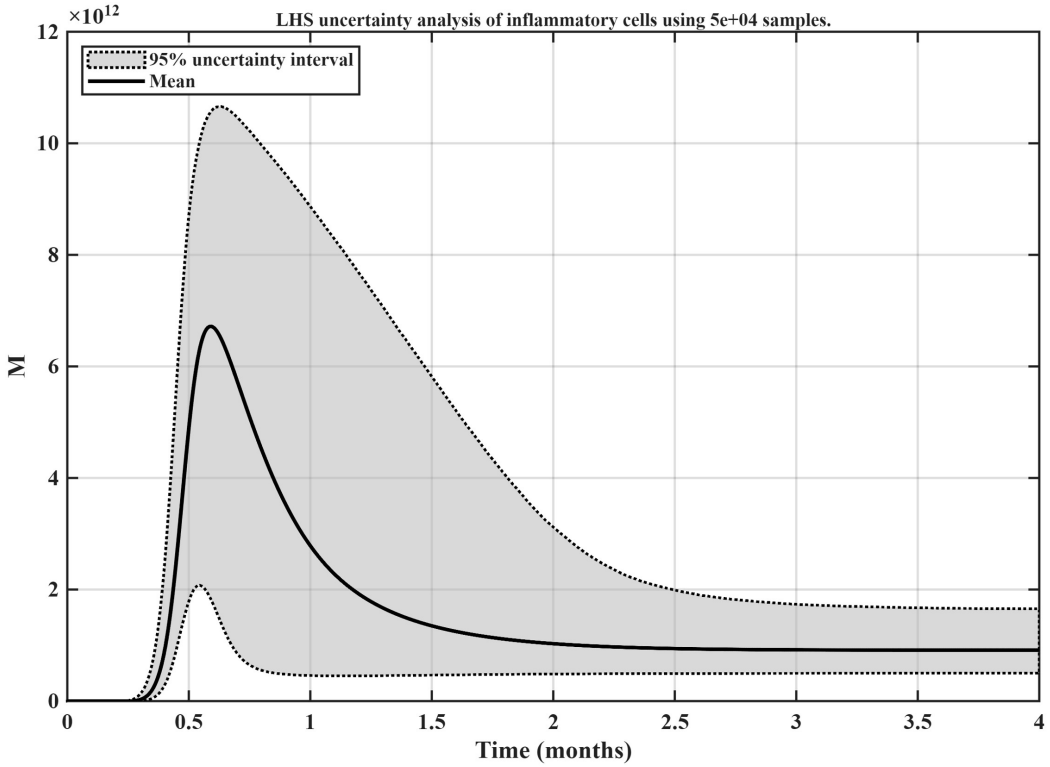

Figure 3. Temporal evolution of inflammatory immune cells (M) for the 5×10^4 LHS sampled parameters.

Figure 3 shows that the inflammatory cell population (M) rises rapidly during the first 0.5–1 month before gradually declining. The initial increase is driven by tumor-induced recruitment and activation of inflammatory cells, whereas the subsequent decrease arises from competition for limited resources and the saturation of tumor-mediated activation mechanisms. The 95% uncertainty interval is initially narrow, then widens, and later narrows again, indicating that the overall pattern of an early inflammatory rise followed by decline remains consistent despite parameter variability.

Overall, the model suggests the following:

- **Early dynamics (first two weeks):** The system is initially dominated by rapid tumor expansion accompanied by a strong inflammatory immune response. This pattern is supported by recent research demonstrating that early stages of lung cancer may be driven by inflammation, with pro-inflammatory activity being particularly pronounced during early phases of tumor development [36, 16]. These findings highlight the potential benefit of early therapeutic interventions targeting pro-inflammatory pathways, consistent with the suggestions in [36].
- **Intermediate dynamics (weeks 2 to 6):** Following its early peak, the inflammatory response steadily declines. During this phase, tumor growth continues but slows progressively, showing that inflammation promotes early tumor expansion and its withdrawal reduces this stimulus. The decline of inflammation after its peak reflects the transient nature of acute inflammatory responses, consistent with experimental evidence [9, 26]. Normal tissue continues its gradual decline during this period. This intermediate stage represents a transition from inflammation-driven

growth toward later dynamics where other growth-limiting factors may become prominent.

- **Long-term dynamics (week** 6 **to month** 4**):** All variables approach a steady state. The inflammatory response persists at a reduced but sustained level, maintaining stable interaction with the tumor. Normal tissue stabilizes at a lower level and tumor at a sustained elevated size. This late phase represents a stage where the system settles into a persistent state of low inflammation and minimal tumor progression.

The variation in the model solutions shown in Figures 1–3 highlights the need to identify the parameters that most strongly influence the model dynamics. To this end, we apply the PRCC method in the next section.

3.3.3. Global sensitivity analysis using PRCC

PRCC is a sensitivity analysis method that evaluates the strength of the relationship between an input parameter and an output variable while removing the linear effects of other parameters. It extends the concept of correlation by working with rank-transformed data, making it suitable for monotonic relationships commonly encountered in biological models. PRCC values range from -1 to 1, where positive values indicate a direct (positive) association, negative values reflect an inverse (negative) association, and values near zero suggest negligible correlation. Coefficients approaching ± 1 denote increasingly strong monotonic relationships between parameter and output.

Since PRCC assumes a monotonic relationship between input parameters and model outputs, we first constructed scatter plots of the sampled parameters against their corresponding outputs to assess monotonicity. The plots were generated using 5×10^4 LHS realizations, with parameter values varied within the ranges listed in Table 1. Figures 7–9 in the appendix show the resulting relationships between each input parameter and model outputs. Visual inspection reveals either a clear monotonic trend or nearly flat patterns, both of which satisfy the monotonicity requirement for PRCC analysis.

Using the 5×10^4 LHS-generated samples, we computed PRCC values and their corresponding p-values for each model output; the results are presented in Figure 4.

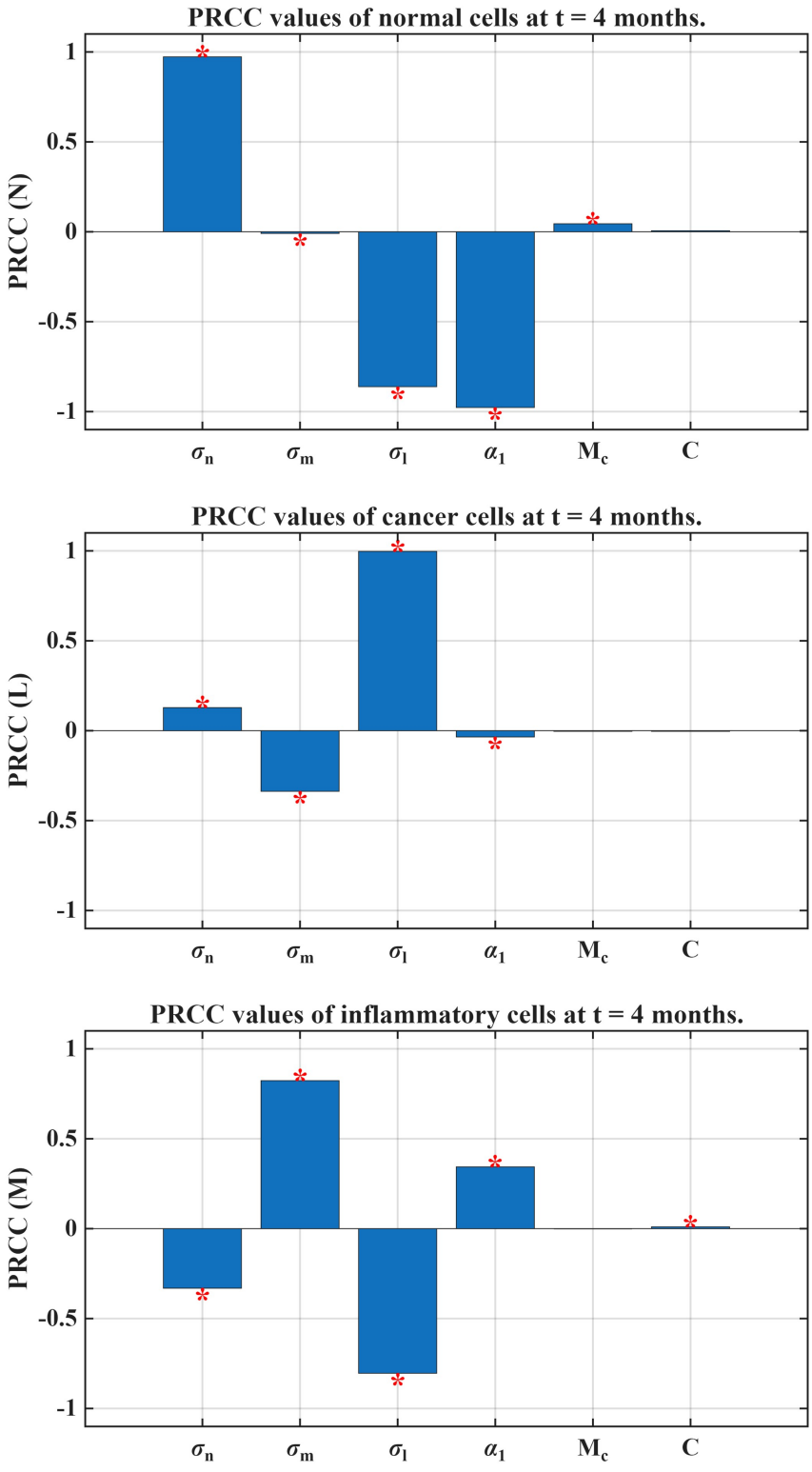

Figure 4. PRCC values obtained from 5×10^4 LHS realizations for the different model outputs. The star indicates the statistical significance threshold $\alpha = 0.05$; PRCC values with $p < 0.05$ are considered statistically significant.

The PRCC values presented in Figure 4 reveal the following biological insights:

i. The parameter σ_n exhibits a strong positive correlation with normal cells, a weak positive correlation with cancer cells, and a weak negative correlation with inflammatory cells. Biologically, σ_n directly promotes normal tissue maintenance through the interaction term $\frac{\sigma_n NM}{C+M}$. Increased normal cells may indirectly support cancer growth via the coupling term $\alpha(M)N$, consistent with evidence that interactions between normal and tumor cells can influence cancer progression [6]. The weak negative association with inflammatory cells likely reflects resource competition within the tumor microenvironment.

ii. The parameter σ_m exhibits a very strong positive correlation with inflammatory cells, a moderate negative correlation with cancer cells, and a very weak correlation with normal tissue. Biologically, this suggests that inflammation may exert an anti-tumor effect without significant collateral damage to normal tissue, which is in line with recent research on targeted inflammatory strategies [30].

iii. The parameter σ_l exhibits a very strong positive correlation with cancer cells, a strong negative correlation with normal cells, and a moderate negative correlation with inflammatory cells. Biologically, this suggests that this pathway is strongly associated with tumor expansion, damage to normal tissue, and reduced inflammatory activity. This represents a scenario where the tumor simultaneously expands, damages surrounding tissue, and actively suppresses the inflammatory response that might otherwise control it, consistent with the findings in [14].

iv. The parameter a_1 exhibits a very strong negative correlation with normal cells and weak to very weak correlations with cancer and inflammatory cells. The strong negative association reflects depletion of normal cells through malignant transformation involving the parameter a_1. The weak effect on cancer cells likely arises because this parameter primarily acts during the early transformation stage.

v. M_c shows negligible to very weak positive effects across all outputs. The transformation threshold acts as a minor delaying factor rather than a strong regulator of final cell counts.

vi. C demonstrates weak positive effect on cancer cells. The saturation constant plays a minimal role in modulating outcomes, indicating low system sensitivity to saturation effects within tested ranges.

The PRCC analysis identifies three immunologically distinct pathways with contrasting therapeutic profiles. Parameter σ_m drives a protective anti-tumor response: it strongly promotes inflammatory cells that suppress cancer while sparing normal tissue. In contrast, σ_l drives tumor expansion and normal tissue damage while dampening inflammatory activity, suggesting a pathogenic role. Meanwhile, σ_n supports normal tissue maintenance but indirectly fuels cancer growth through coupling terms and may limit inflammatory cells via resource competition.

These findings carry clear therapeutic implications. Strategies should aim to harness the σ_m pathway to enhance anti-tumor immunity without toxicity. Conversely, σ_l represents a potential target for inhibition, as it is associated with tumor progression, tissue damage, and reduced inflammation. The dual role of σ_n highlights the challenge of supporting healthy tissue without promoting cancer.

Finally, to determine whether parameter influences vary across different phases of tumor-immune dynamics, we tracked the evolution of PRCC values and their significance levels over the full simulation timeframe. The results are shown in Figure 5.

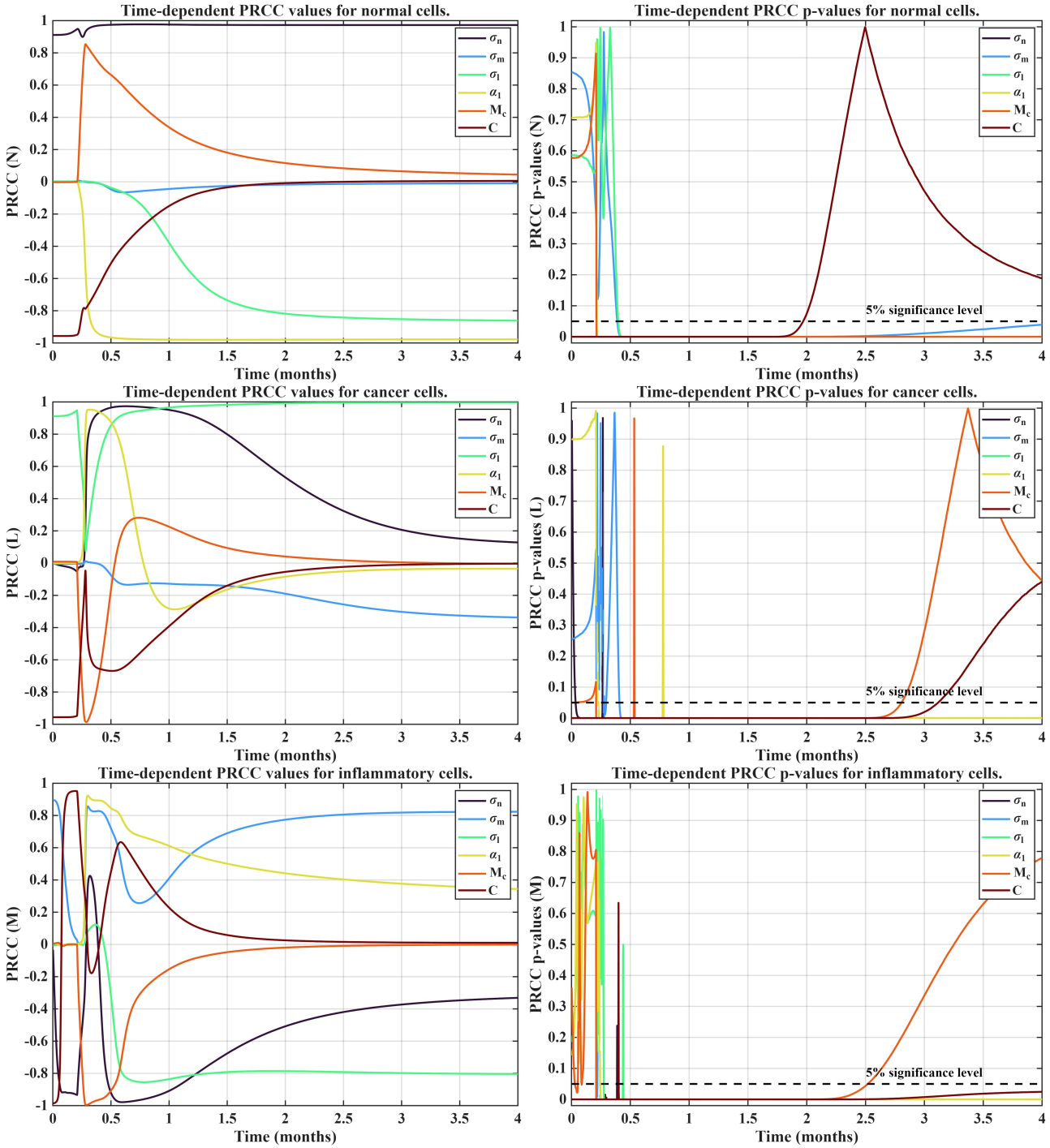

Figure 5. Temporal PRCC and their associated p-values obtained from 5×10^4 LHS realizations for the different model outputs. The dashed horizontal line indicates the statistical significance threshold; PRCC values with $p < 0.05$ are considered statistically significant.

Inspection of Figure 5 reveals that most parameters are not statistically significant during the first two weeks. The relatively large p-values observed during this initial period arise because the early dynamics are primarily governed by the prescribed initial conditions and intrinsic growth processes. During this transient regime, key mechanisms, such as inflammatory amplification, remain weak and only become influential once the tumor burden has sufficiently increased. Moreover, nonlinear interaction terms, such as $\frac{NM}{C+M}$, remain negligible while M is low. As a result, the associated parameters exert little significant effect until the system evolves away from its initial state. Beyond this period, significance is attained for the majority of the parameters, except C for normal cells, M_c for inflammatory cells, and both M_c and C for cancer cells. Accordingly, our interpretation focuses on PRCC values from the first two weeks onward.

The PRCC values over the period $0.5 - 4$ months presented in Figure 5 reveal the following biological insights:

- σ_n: Exerts a consistently strong protective effect on normal cells throughout the simulation. It also shows a strong promoting effect on cancer cells that gradually declines over time and a decreasing negative effect on inflammatory cells, suggesting its influence on the immune compartment weakens progressively.
- σ_m: Demonstrates a consistently weak negative effect on normal cells, indicating mild collateral damage. It exhibits a weak but strengthening anti-tumor effect over time. Its positive effect on inflammatory cells increases over time.
- σ_l: Displays moderate and progressively increasing negative effect on normal cells. It remains a consistently strong driver of cancer cell proliferation across all time points and has a consistently strong negative effect on inflammatory cells.
- α_1: Shows a consistent and negative effect on normal cells reflecting depletion of the normal cells via transformation to cancer cells. It has a weak negative effect on cancer cells suggesting that this transformation alone does not substantially amplify tumor burden. Instead, cancer cells may be driven by other mechanisms, such as intrinsic proliferation or inflammation-driven growth. Its positive effect on inflammatory cells decreases over time, implying that the immune response triggered by conversion wanes as the tumor progresses.
- M_c: Exhibits a statistically significant weak positive effect on normal cells. It also shows a statistically significant weak positive effect on cancer cells up to approximately month 3, after which the effect becomes statistically non-significant due to larger p-values, indicating that delayed immune activation may initially permit tumor growth. A similar pattern is observed for inflammatory cells, except that the effect is negative rather than positive.
- C: Exerts a weak negative effect on both normal and cancer cells that remains statistically significant for 2 and 3 months, respectively. Its protective effect on cancer cells also declines to negligible levels. For inflammatory cells, it has a statistically significant weak positive effect that decays over time.

4. Discussion and concluding remarks

Mathematical modeling of cancer-inflammation dynamics remains an underexplored yet critically important area, given the growing recognition of inflammation as both a driver and a regulator of tumor

progression. While existing models have laid valuable groundwork, they are relatively few and often do not capture the full complexity of interactions between cancer cells, inflammatory cells, and normal tissue. The present study contributes to this emerging field by proposing a simple but mechanistically grounded model consisting of three ordinary differential equations that track these populations and their interactions.

We performed a steady-state and stability analysis revealing that inflammation will emerge and be established over time and has the potential to destabilize the cancer-free equilibrium, potentially enabling the initiation of cancer. However, while inflammation may emerge, it can only persist when microenvironmental resources are sufficient to sustain it above the critical threshold M_c; below this threshold, any inflammatory response inevitably subsides.

To account for parameter variability, we performed an uncertainty analysis using LHS. This revealed three distinct dynamical phases consistent with recent findings [36, 16, 9, 26]. In the early phase, rapid tumor expansion is accompanied by a strong inflammatory immune response, highlighting the potential benefit of early interventions targeting pro-inflammatory pathways. During the intermediate phase, inflammation steadily declines while tumor growth continues but slows progressively, reflecting the transient nature of acute inflammatory responses. In the long term, all variables approach a steady state where inflammation persists at a reduced but sustained level, maintaining stable interaction with the tumor.

The PRCC sensitivity analysis revealed three immunologically distinct pathways with direct therapeutic relevance.

- One pathway, associated with inflammatory activation, promotes anti-tumor immunity by enhancing inflammatory cells that suppress cancer while sparing normal tissue. This suggests that therapeutic strategies aimed at boosting this protective inflammatory response could yield selective anti-tumor effects without significant collateral damage to normal tissue.
- A second pathway, linked to tumor growth, drives cancer expansion and normal tissue destruction while simultaneously dampening inflammatory activity. This pathogenic profile supports the rationale for inhibiting such pathways using targeted therapies that block tumor-promoting signals and restore immune responsiveness.
- A third pathway, involved in normal tissue maintenance, presents a therapeutic challenge: while supporting healthy tissue is essential, it may inadvertently fuel cancer growth through indirect coupling mechanisms and resource competition. This highlights the need for carefully balanced interventions that preserve normal tissue function without creating conditions that favor tumor progression.

These findings highlight the dual role of inflammation in cancer, both tumor-suppressive and tumor-promoting, and identifies distinct therapeutic strategies. Boosting beneficial inflammatory pathways while blocking tumor-promoting ones may offer a promising approach to treatment. However, the complex interactions between inflammation, tumor growth, and normal tissue require further experimental validation. By combining mathematical modeling with biological insight, this study provides a foundation for understanding and targeting inflammation in cancer.

5. Appendix

In this appendix, we present the center manifold reduction and illustrate pairwise associations between sampled parameters, as well as monotonic trends between input parameters and output variables.

5.1. Center manifold reduction

We start by recalling the center manifold theorem

Theorem 8 (Local center manifold theorem)**.** *[45] Let $f \in C^r(E)$, where E is an open subset of $\mathbb{R}^n$ containing the origin and $r \geq 1$. Suppose that $f(0) = 0$ and that $Df(0)$ has c eigenvalues with zero real part and $s = n - c$ eigenvalues with negative real part. Then, the system*

$$\frac{d}{dt}\begin{pmatrix} x \\ y \end{pmatrix} = f(x, y) \tag{5.1}$$

can be transformed into the following diagonal form:

$$\begin{aligned} \dot{x} &= Cx + F(x, y), \\ \dot{y} &= Py + G(x, y), \end{aligned} \tag{5.2}$$

where $(x, y) \in \mathbb{R}^c \times \mathbb{R}^s$, C is a $c \times c$ matrix whose eigenvalues have zero real parts, P is an $s \times s$ matrix whose eigenvalues have negative real parts, and $F(0, 0) = G(0, 0) = 0$, $DF(0, 0) = DG(0, 0) = 0$.

Moreover, there exists $\delta > 0$ and a function $h \in C^r(N(0))$ with $h(0) = 0$, $Dh(0) = 0$, defined on a neighborhood $N(0)$ of the origin in $\mathbb{R}^c$, such that the local center manifold is given by

$$W^c(0) := \{(x, y) \in \mathbb{R}^c \times \mathbb{R}^s \mid y = h(x),\ \|x\| < \delta\}$$

and satisfies the following invariance equation:

$$Dh(x)[Cx + F(x, h(x))] = Ph(x) + G(x, h(x)), \quad \text{for } \|x\| < \delta.$$

The flow on the center manifold $W^c(0)$ is governed by the following reduced system:

$$\dot{x} = Cx + F(x, h(x)), \quad \text{for all } x \in \mathbb{R}^c \text{ with } \|x\| < \delta.$$

To apply this theorem to system (2.1), we first rewrite it in canonical form by shifting the equilibrium point to the origin and then diagonalizing the resulting system. This is achieved through the change of variables

$$y = T^{-1}\left((N, L, M) - E_n\right),$$

where T is the matrix that diagonalizes the Jacobian at E_n, that is,

$$J_{E_n} = T \triangle T^{-1},$$

with

$$T = \begin{bmatrix} \dfrac{K\sigma_n + CKr_n\rho'(K)}{-CKr_n\rho'(K)} & -1 & 1 \\ 0 & 1 & 0 \\ 1 & 0 & 0 \end{bmatrix}, \quad \triangle = \begin{bmatrix} 0 & 0 & 0 \\ 0 & 0 & 0 \\ 0 & 0 & Kr_n\rho'(K) \end{bmatrix}.$$

The resulting system reads as

$$x' = T^{-1} f\,(Tx + E_n)$$

where f denote the right hand side of model (2.1).
Using Maple software, we obtain the following system:

$$\left\{\begin{array}{rcl} x_1' &=& g_1(x_1, x_2, x_3) \\ x_2' &=& g_2(x_1, x_2, x_3) \\ x_3' &=& -r_n x_3 + g_3(x_1, x_2, x_3) \end{array}\right. \tag{5.3}$$

where

$$\left\{\begin{array}{l} g_1(x) = -\frac{1}{-KKr_n\rho'(K)C(C+x_1)}\Big(x_1\big(-C^2r_mKr_n\rho'(K)x_3 + CKr_mx_1\sigma_n + CKKr_n\rho'(K)x_2\sigma_m - Cr_mKr_n\rho'(K)x_1x_3 + Kr_mx_1^2\sigma_n\big)\Big) \\ g_2(x) = -\frac{1}{-KKr_n\rho'(K)C(C+x_1)}\Big(x_2\big(-C^2r_lKr_n\rho'(K)x_3 + CKr_lx_1\sigma_n + CKKr_n\rho'(K)x_1\sigma_l - Cr_lKr_n\rho'(K)x_1x_3 + Kr_lx_1^2\sigma_n\big)\Big) \\ g_3(x) = \frac{1}{(Kr_n\rho'(K))^2C^2K(C+x_1)}\left(\begin{array}{l} C^3K^2(-Kr_n\rho'(K))^3 - C^3r_l(Kr_n\rho'(K))^2x_2x_3 - C^3r_m(Kr_n\rho'(K))^2x_1x_3 + C^3(-Kr_n\rho'(K))^3x_1x_3 + C^3(-Kr_n\rho'(K))^3x_2x_3 \\ -C^3(-Kr_n\rho'(K))^3x_3^2 + C^2K^2(-Kr_n\rho'(K))^3x_1 - C^2Kr_l(-Kr_n\rho'(K))x_1x_2\sigma_n - C^2Kr_m(-Kr_n\rho'(K))x_1^2\sigma_n \\ +C^2Kr_m(-Kr_n\rho'(K))x_1x_3\sigma_n + C^2K(-Kr_n\rho'(K))^2x_1x_2\sigma_l + C^2K(-Kr_n\rho'(K))^2x_1x_2\sigma_m - C^2K(-Kr_n\rho'(K))^2x_1x_3\sigma_n \\ -C^2r_l(-Kr_n\rho'(K))^2x_1x_2x_3 - C^2r_m(-Kr_n\rho'(K))^2x_1^2x_3 + C^2(-Kr_n\rho'(K))^3x_1^2x_3 + C^2(-Kr_n\rho'(K))^3x_1x_2x_3 \\ -C^2(-Kr_n\rho'(K))^3x_1x_3^2 + CK^2r_mx_1^2\sigma_n^2 - CK^2(-Kr_n\rho'(K))^2x_1^2\sigma_n - CK^2(-Kr_n\rho'(K))x_1x_2\sigma_m\sigma_n \\ -CKr_l(-Kr_n\rho'(K))x_1^2x_2\sigma_n - CKr_m(-Kr_n\rho'(K))x_1^3\sigma_n + CKr_m(-Kr_n\rho'(K))x_1^2x_3\sigma_n \\ +CK(-Kr_n\rho'(K))^2x_1^3\sigma_n + CK(-Kr_n\rho'(K))^2x_1^2x_2\sigma_n - 2CK(-Kr_n\rho'(K))^2x_1^2x_3\sigma_n + K^2r_mx_1^3\sigma_n^2 - K^2(-Kr_n\rho'(K))x_1^3\sigma_n^2 \end{array}\right) \end{array}\right.$$

By the center manifold theorem there exists a center manifold $y = h(x)$ for (5.3), and the reduced system on this manifold

$$\left\{\begin{array}{l} x_1' = g_1(x_1, x_2, h(x_1, x_2)) \\ x_2' = g_2(x_1, x_2, h(x_1, x_2)) \end{array}\right. \tag{5.4}$$

governs the dynamics of (5.3) near $(x_1, x_2) = (0, 0)$. The manifold h is not unique, but its Taylor expansion to any finite order is. Using the invariance condition

$$D_1h(x_1, x_2)x_1' + D_2h(x_1, x_2)x_2' = -r_nh(x_1, x_2) + g_3(x_1, x_2, h(x_1, x_2)),$$

and imposing $h(0, 0) = 0$, $Dh(0, 0) = 0$, we seek a center manifold

$$h(x_1, x_2) = a_{11}x_2^2 + a_{12}x_1x_2 + a_{13}x_1^2.$$

Equating second–order terms in the invariance equation yields the coefficients a_{ij}. Substituting these into the reduced system (5.4) yields

$$\left\{\begin{array}{l} x_1' = \dfrac{x_1\left(-Kr_n\rho'(K)\sigma_mx_2 - r_m\sigma_nx_1\right)}{-Kr_n\rho'(K)(C + x_1)} \\ x_2' = \dfrac{x_1x_2\left(-Kr_n\rho'(K)\sigma_l - r_l\sigma_n\right)}{-Kr_n\rho'(K)(C + x_1)} \end{array}\right. \tag{5.5}$$

5.2. LHS

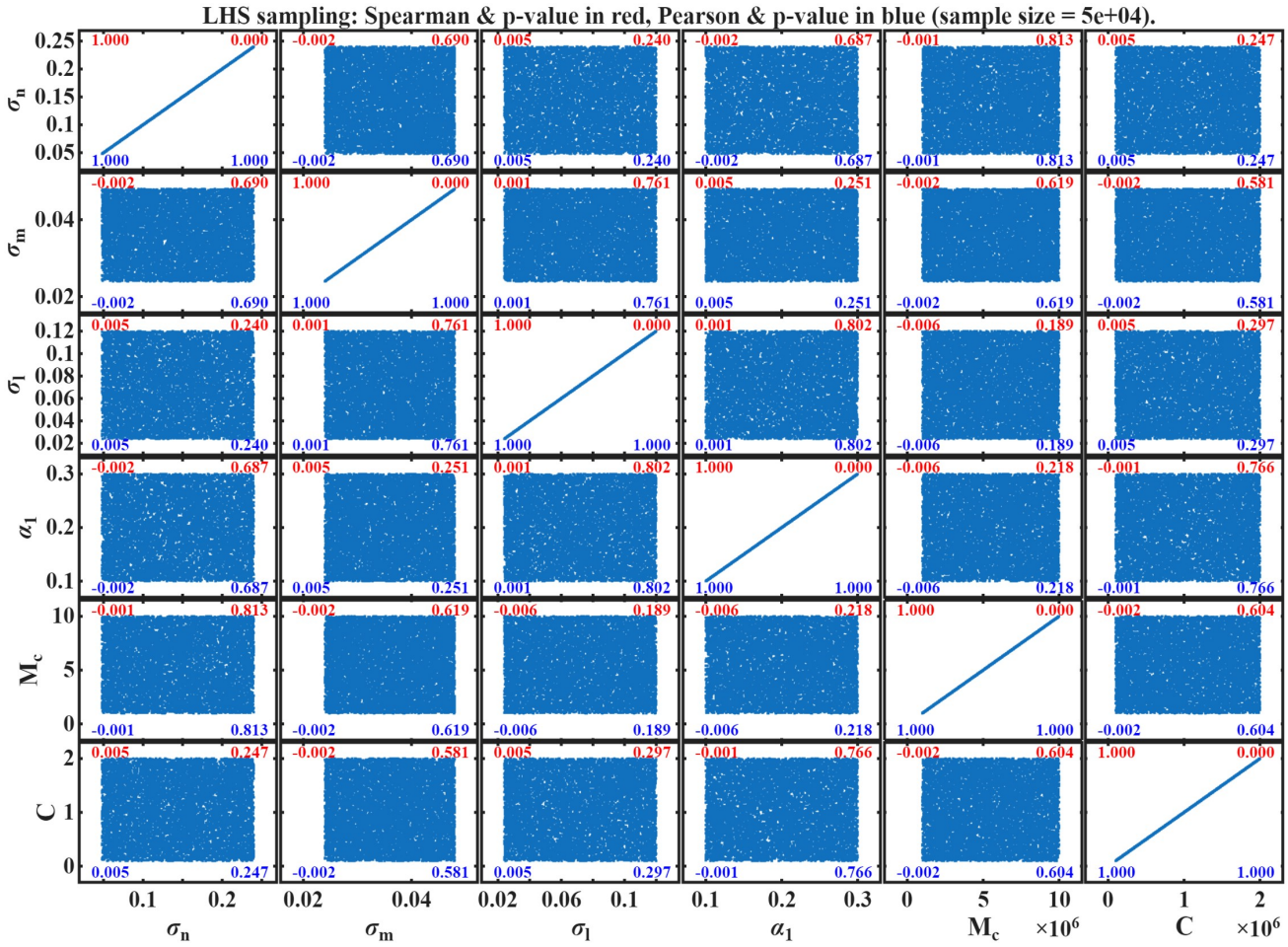

Figure 6. Pairwise scatter plots of the 5×10^4 LHS realizations of the model's parameters. Pearson (blue) and Spearman (red) correlation coefficients are displayed on the left of each panel, with the corresponding p-values on the right. The off-diagonal panels show negligible correlations, indicating that the LHS design preserves near-independence among the sampled parameters.

5.3. *Scatter plots for monotonicity test*

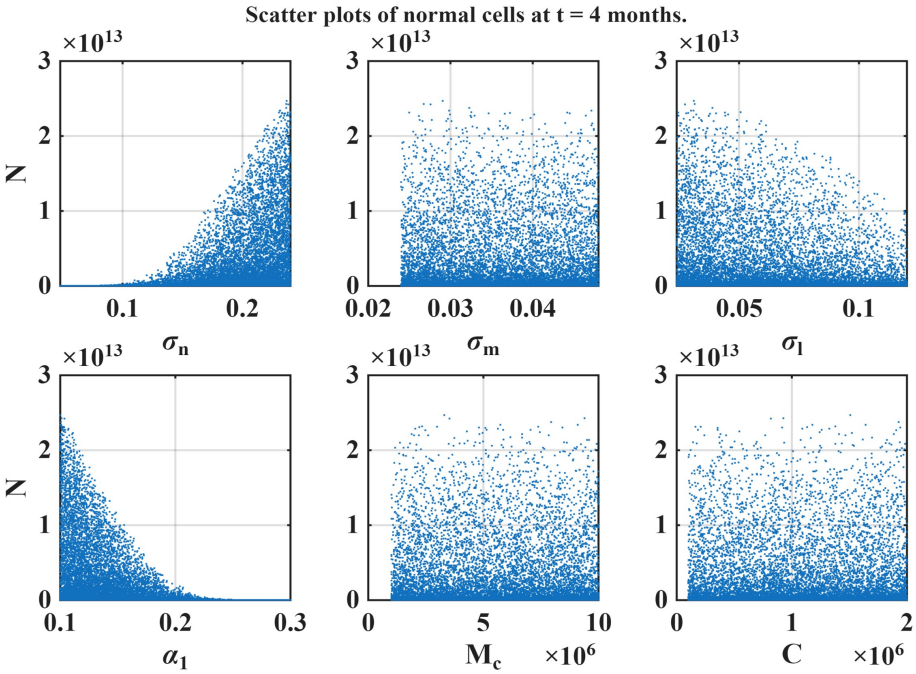

Figure 7. Scatter plots of normal cells (N) at time 4 months with respect to each input parameter.

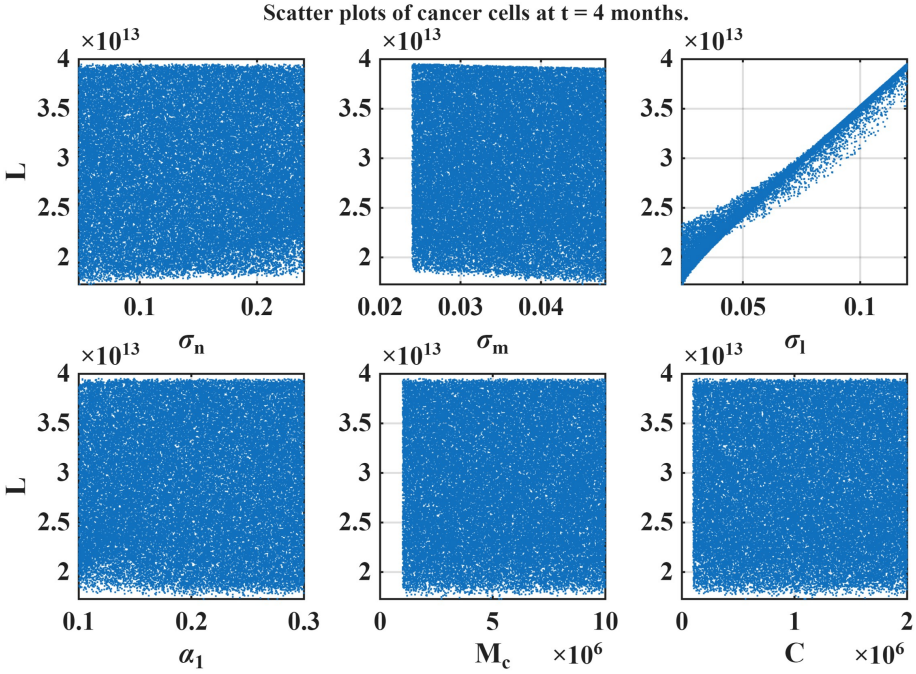

Figure 8. Scatter plots of cancer cells (L) at time 4 months with respect to each input parameter.

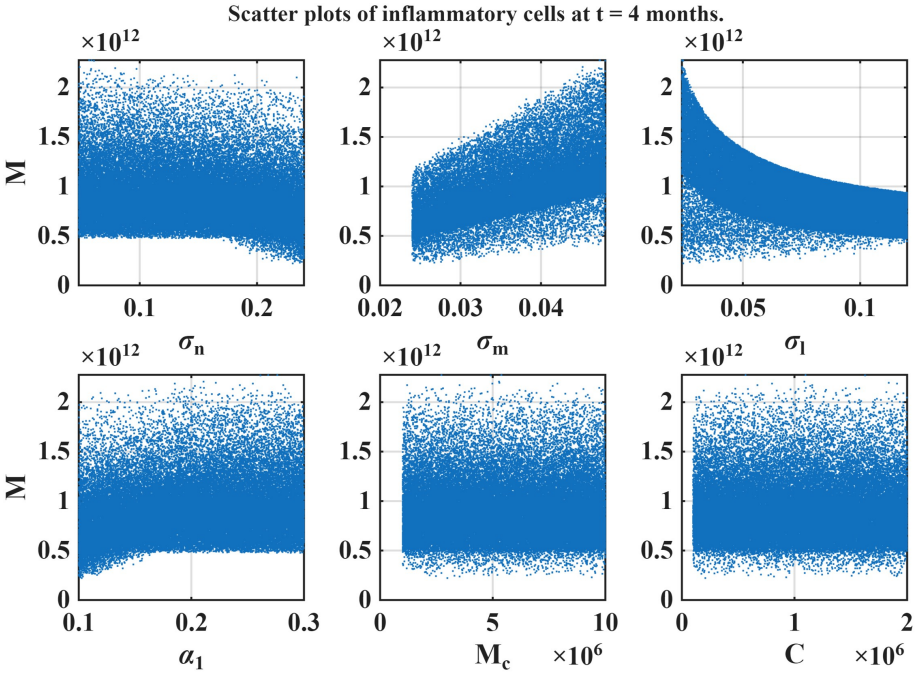

Figure 9. Scatter plots of inflammatory immune cells (M) at time 4 months with respect to each input parameter.

Use of AI tools declaration

The authors declare they have not used Artificial Intelligence (AI) tools in the creation of this article.

Acknowledgments

R. Ouifki acknowledges the support from the research entity Pure and Applied Analytics, North-West University and the DST/NRF SARChI Chair in Mathematical Models and Methods in Biosciences and Bioengineering, University of Pretoria. E. Afenya acknowledges the support from the Faculty Research Grants Program of Elmhurst University.

Conflict of interest

The authors declare there is no conflict of interest.

References

1. E. K. Afenya, Recovery of normal hemopoiesis in disseminated cancer therapy–a model, *Math. Biosci.*, **172** (2001), 15–32. https://doi.org/10.1016/S0025-5564(01)00061-X
2. E. K. Afenya, S. D. Mundle, Hematologic disorders and bone marrow–peripheral blood dynamics, *Math. Model. Nat. Pheno.*, **5** (2010), 15–27. https://doi.org/10.1051/mmnp/20105302
3. E. K. Afenya, R. Ouifki, B. I. Camara, S. D. Mundle, Mathematical modeling of bone marrow–

peripheral blood dynamics in the disease state based on current emerging paradigms, part I. *Math. Biosci.*, **274** (2016), 83–93. https://doi.org/10.1016/j.mbs.2016.01.010

4. E. K. Afenya, R. Ouifki, S. D. Mundle, Mathematical modeling of bone marrow–peripheral blood dynamics in the disease state based on current emerging paradigms, part II, *J. Theor. Biol.*, **460** (2019), 37–55. https://doi.org/10.1016/j.jtbi.2018.10.008
5. M. Al-Hajj, M. S. Wicha, A. Benito-Hernandez, S. J. Morrison, M. F. Clarke, Prospective identification of tumorigenic breast cancer cells, *Proceed. Nat. Acad. Sci.*, **100** (2003), 3983–3988. https://doi.org/10.1073/pnas.0530291100
6. A. Amrenova, K. Suzuki, V. Saenko, S. Yamashita, N. Mitsutake, Cell competition between anaplastic thyroid cancer and normal thyroid follicular cells exerts reciprocal stress response defining tumor suppressive effects of normal epithelial tissue, *PLoS ONE*, **16** (2021), e0249059. https://doi.org/10.1371/journal.pone.0249059
7. M. Andersen, Z. Sajid, R. K. Pedersen, J. Gudmand-Hoeyer, C. Ellervik, V. Skov, et al., Mathematical modelling as a proof of concept for MPNs as a human inflammation model for cancer development, *PLoS ONE*, **12** (2017), e0183620. https://doi.org/10.1371/journal.pone.0183620
8. N. Behranvand, F. Nasri, R. Zolfaghari Emameh, P. Khani, A. Hosseini, J. Garssen, et al., Chemotherapy: A double-edged sword in cancer treatment, *Cancer Immunol. Immunother.*, **71** (2022), 507–526. https://doi.org/10.1007/s00262-021-03013-3
9. Q. Bi, J.-Y. Wu, X.-M. Qiu, J.-D. Zhang, Z.-J. Sun, W. Wang, Tumor-associated inflammation: The tumor-promoting immunity in the early stages of tumorigenesis, *J. Immunol. Res.*, **2022** (2022), 3128933. https://doi.org/10.1155/2022/3128933
10. R. L. Blaylock, Cancer microenvironment, inflammation and cancer stem cells: A hypothesis for a paradigm change and new targets in cancer control, *Surg. Neurol. Int.*, **6** (2015), 92. https://doi.org/10.4103/2152-7806.157890
11. D. Bonnet, J. E. Dick, Human acute myeloid leukemia is organized as a hierarchy that originates from a primitive hematopoietic cell, *Nat. Med.*, **3** (1997), 730–737. https://doi.org/10.1038/nm0797-730
12. S. Demaria, E. Pikarsky, M. Karin, L. M. Coussens, Y.-C. Chen, E. M. El-Omar, et al., Cancer and inflammation: Promise for biologic therapy, *J. Immunother.*, **33** (2010), 335–351. https://doi.org/10.1097/CJI.0b013e3181d32e74
13. D. Dingli, F. Michor, Successful therapy must eradicate cancer stem cells, *Stem Cells*, **24** (2006), 2603–2610. https://doi.org/10.1634/stemcells.2006-0136
14. G. P. Dunn, L. J. Old, R. D. Schreiber, The Three Es of Cancer Immunoediting, *Annu. Rev. Immunol.*, **22** (2004), 329–360. https://doi.org/10.1146/annurev.immunol.22.012703.104803
15. J. L. Dunster, H. M. Byrne, J. R. King, The resolution of inflammation: A mathematical model of neutrophil and macrophage interactions, *Bull. Math. Biol.*, **76** (2014), 1953–1980. https://doi.org/10.1007/s11538-014-9987-x
16. American Association for Cancer Research, Early proinflammatory niches drive lung adenocarcinoma initiation, *Cancer Discov.*, **16** (2026), OF1. https://doi.org/10.1158/2159-8290.CD-RW2025-108

17. R. J Gilbertson, J. N. Rich, Making a tumour's bed: Glioblastoma stem cells and the vascular niche, *Nat. Rev. Cancer*, **7** (2007), 733–736. https://doi.org/10.1038/nrc2246

18. S. I. Grivennikov, F. R. Greten, M. Karin, Immunity, inflammation, and cancer, *Cell*, **140** (2010), 883–899. https://doi.org/10.1016/j.cell.2010.01.025

19. D. Hanahan, R. A. Weinberg, Hallmarks of Cancer: The Next Generation, *Cell*, **144** (2011), 646–674. https://doi.org/10.1016/j.cell.2011.02.013

20. S. Hibino, T. Kawazoe, H. Kasahara, S. Itoh, T. Ishimoto, M. Sakata-Yanagimoto, et al., Inflammation-induced tumorigenesis and metastasis, *Int. J. Molecular Sci.*, **22** (2021), 5421. https://doi.org/10.3390/ijms22115421

21. Y. J. Jeong, H. K. Oh, S. H. Park, J. G. Bong, Association between inflammation and cancer stem cell phenotype in breast cancer, *Oncol. Lett.*, **15** (2018), 2380–2386. https://doi.org/10.3892/ol.2017.7607

22. M. Karin, Nuclear factor-κb in cancer development and progression, *Nature*, **441** (2006), 431–436. https://doi.org/10.1038/nature04870

23. H. Kulbe, T. Hagemann, P. W. Szlosarek, F. R. Balkwill, J. L. Wilson, The inflammatory cytokine tumor necrosis factor-α regulates chemokine receptor expression on ovarian cancer cells, *Cancer Res.*, **65** (2005), 10355–10362. https://doi.org/10.1158/0008-5472.CAN-05-0957

24. P. La Rosée, A. Horne, M. Hines, T. von B. Greenwood, R. Machowicz, N. Berliner, et al., Recommendations for the management of hemophagocytic lymphohistiocytosis in adults, *Blood*, **133** (2019), 2465–2477. https://doi.org/10.1182/blood.2018894618

25. H. T. Lu, W. M. Ouyang, C. S. Huang, Inflammation, a key event in cancer development, *Mol. Cancer Res.*, **4** (2006), 221–233. https://doi.org/10.1158/1541-7786.MCR-05-0261

26. Y. M. Ma, T. Sun, Y. X. Liu, N. Zhao, Q. Gu, D.-F. Zhang, et al., A pilot study on acute inflammation and cancer: A new balance between IFN-γ and TGF-β in melanoma, *J. Exp. Clin. Canc. Res.*, **28** (2009), 1–6. https://doi.org/10.1186/1756-9966-28-23

27. A. Mantovani, P. Allavena, A. Sica, F. Balkwill, Cancer-related inflammation, *Nature*, **454** (2008), 436–444. https://doi.org/10.1038/nature07205

28. S. Marino, I. B. Hogue, C. J. Ray, D. E. Kirschner, A methodology for performing global uncertainty and sensitivity analysis in systems biology, *J. Theor. Biol.*, **254** (2008), 178–196. https://doi.org/10.1016/j.jtbi.2008.04.011

29. M. D. McKay, R. J. Beckman, W. J. Conover, A comparison of three methods for selecting values of input variables in the analysis of output from a computer code, *Technometrics*, **21** (1979), 239–245. https://doi.org/10.1080/00401706.1979.10489755

30. S. Mohapatra, A. Guerrero, N. Rahman, K. T. Zaman, J. Wu, C. Onyeagba, et al., Novel taxol-derivative, sto-1, induces selective anti-tumor immunity and sustained remission of glioblastoma without triggering autoimmune reactions, *Cells*, **14** (2025), 1703. https://doi.org/10.3390/cells14211703

31. T.-N. Nguyen, J. Clairambault, T. Jaffredo, B. Perthame, D. Salort, Adaptive dynamics of hematopoietic stem cells and their supporting stroma: a model and mathematical analysis, *Math. Biosci. Eng.*, **16** (2019), 4818–4845. https://doi.org/10.3934/mbe.2019243

32. L. Norton, R. Simon, The norton-simon hypothesis revisited, *Cancer Treat. Rep.*, **70** (1986), 163–169.

33. F. Okada, Inflammation and free radicals in tumor development and progression, *Redox Rep.*, **7** (2002), 357–368. https://doi.org/10.1179/135100002125001135

34. J. T. Ottesen, R. K. Pedersen, Z. Sajid, J. Gudmand-Hoeyer, K. O. Bangsgaard, V. Skov, et al., Bridging blood cancers and inflammation: The reduced cancitis model, *J. Theor. Biol.*, **465** (2019), 90–108. https://doi.org/10.1016/j.jtbi.2019.01.001

35. K. Pearson, VII. Note on regression and inheritance in the case of two parents, *Proceed. Royal Soc. London*, **58** (1895), 240–242. https://doi.org/10.1098/rspl.1895.0041

36. F. Peng, A. Sinjab, Y. Dai, W. Treekitkarnmongkol, S. Yang, L. I. G. Bolanos, et al., Multimodal spatial-omics reveal co-evolution of alveolar progenitors and proinflammatory niches in progression of lung precursor lesions, *Cancer Cell*, **44** (2026), 321–339. https://doi.org/10.1016/j.ccell.2025.10.004

37. E. M. Pietras, Inflammation: A key regulator of hematopoietic stem cell fate in health and disease, *Blood*, **130** (2017), 1693–1698. https://doi.org/10.1182/blood-2017-06-780882

38. C. Récher, Clinical implications of inflammation in acute myeloid leukemia, *Front. Oncol.*, **11** (2021), 623952. https://doi.org/10.3389/fonc.2021.623952

39. T. Reya, S. J. Morrison, M. F. Clarke, I. L. Weissman, Stem cells, cancer, and cancer stem cells, *Nature*, **414** (2001), 105–111. https://doi.org/10.1038/35102167

40. Z. Sajid, M. Andersen, J. T. Ottesen, Mathematical analysis of the cancitis model and the role of inflammation in blood cancer progression, *Math. Biosci. Eng.*, **16** (2019), 8268–8289. https://doi.org/10.3934/mbe.2019418

41. A. M. Schram, N. Berliner, How I treat hemophagocytic lymphohistiocytosis in the adult patient, *Blood*, **125** (2015), 2908–2914. https://doi.org/10.1182/blood-2015-01-551622

42. S. Shigdar, Y. Li, S. Bhattacharya, M. O'Connor, C. Pu, J. Lin, et al., Inflammation and cancer stem cells, *Cancer Lett.*, **345** (2014), 271–278. https://doi.org/10.1016/j.canlet.2013.07.031

43. A. Sparmann, D. Bar-Sagi, Ras-induced interleukin-8 expression plays a critical role in tumor growth and angiogenesis, *Cancer Cell*, **6** (2004), 447–458. https://doi.org/10.1016/j.ccr.2004.09.028

44. C. Spearman, The proof and measurement of association between two things, (1961). https://doi.org/10.1037/11491-005

45. S. Wiggins, *Introduction to applied nonlinear dynamical systems and chaos*, Springer, 2003.

46. C. Y. Huak, Biostatistics 104: Correlational Analysis, *Singapore Med. J.*, **44** (2003), 614–619.

47. Y. Zhang, W. Sime, M. Juhas, A. Sjölander, Crosstalk between colon cancer cells and macrophages via inflammatory mediators and cd47 promotes tumour cell migration, *Eur. J. Cancer*, **49** (2013), 3320–3334. https://doi.org/10.1016/j.ejca.2013.06.005

AIMS Press